

Article

Prototype Experiments Assessing Arsenic and Iron Removal Efficiencies through Adsorption Using Natural Skye Sand

Shahnour Alam Khan ¹ and Monzur Alam Imteaz ^{2,*} ¹ School of Chemistry, Monash University, Clayton, VIC 3800, Australia² Department of Civil & Construction Engineering, Swinburne University of Technology, Melbourne, VIC 3122, Australia

* Correspondence: mimteaz@swin.edu.au

Abstract: Based on earlier batch and column experimental results, it was established that Skye sand is suitable for removing arsenic from water through adsorption. As a real-size prototype may not always replicate results from batch and column experiments, this paper presents experimental results on arsenic removal through a prototype arsenic filter using the same Skye sand used in the batch and column experiments. As arsenic-contaminated water is often associated with a high concentration of iron, which causes blockage of the filter system, this study also investigates the removal of iron from the water through the same filter media. First, several physical properties of the Skye sand were established through XRF, XRD, SEM and EDX analyses. Then, a real-size prototype was made based on an earlier design of a similar filter made of iron oxide-coated sand (IOCS). It was found that the current filter is capable of removing arsenic consistently to a level below the detection limit (0.05 µg/L) for a considerable period (up to 150 bed volumes). Additionally, the same filter is capable of removing iron to a level below the WHO-acceptable limit (0.3 mg/L). Analytical calculation suggests that the current prototype filter with Skye sand can produce arsenic-free water continuously for 600 days (100 L per day) with a feed arsenic concentration of 500 µg/L.

Keywords: Skye sand; iron; arsenic; IOCS

Citation: Khan, S.A.; Imteaz, M.A. Prototype Experiments Assessing Arsenic and Iron Removal Efficiencies through Adsorption Using Natural Skye Sand. *Water* **2023**, *15*, 785. <https://doi.org/10.3390/w15040785>

Academic Editor: Alexandre T. Paulino

Received: 28 January 2023

Revised: 12 February 2023

Accepted: 16 February 2023

Published: 17 February 2023



Copyright: © 2023 by the authors. Licensee MDPI, Basel, Switzerland. This article is an open access article distributed under the terms and conditions of the Creative Commons Attribution (CC BY) license (<https://creativecommons.org/licenses/by/4.0/>).

1. Introduction

In different parts of the world, arsenic contamination in drinking water has become a critical issue and a cause of safety concern for the relevant health and water authorities as many of those places do not have an alternate source of potable water. The World Health Organisation (WHO) has set the limit of arsenic contamination at 10 µg/L for drinking water [1]. Continuous long-term exposure and consumption of water with a concentration of arsenic higher than the above-mentioned limit may cause several health hazards such as skin diseases, pigmentation, neurological disorders and cancer [2]. In general, arsenic in natural water can be present as both organic and inorganic forms; however, its inorganic form is more toxic to humans and the environment. As arsenic exhibits high reactivity with oxygen, in the presence of oxygen, arsenic in the water converts to inorganic arsenic such as pentavalent arsenate, As (V), and trivalent arsenite, As (III) [3]. As such, most common inorganic forms of arsenic in natural water are As (III) and As (V), proportions of which depend on the redox potential and the pH of water [4].

As this is a major concern and health hazard for communities where source(s) of available water are contaminated with arsenic, in the past, various physicochemical techniques have been proposed and implemented for the removal of arsenic from water to be used for human consumption [5–11]. Different researchers have applied different methods and each method was investigated using different materials. Many of those methods were applied not only for arsenic, but also for other pollutants. For example, Sakr et al. [5] investigated the adsorption of uranium from wastewater using nano-silica/chitosan and

achieved a maximum uranium adsorption of 165 mg per gram of adsorbent. Boussouga et al. [6] investigated the removal of arsenic using membrane technology (nanofiltration) and achieved up to 94% removal of As (V). Goren and Kobya [7] investigated the removal of arsenic through an electrocoagulation technique and achieved a maximum arsenic removal efficiency of 98.6% under optimised conditions. Khan and Imteaz [12] employed adsorption techniques for the remediation of arsenic using natural Skye sand and achieved 90% removal efficiency with a very high initial concentration (500 µg/L) of arsenic. Bora et al. [8] used a combined oxidation–coagulation technique for the effective removal of arsenic from water and demonstrated the removal of arsenic to less than 2 µg/L (undetectable) from an initial concentration of 100 µg/L. Recently, Xiong et al. [13] used schwertmannites (an iron-oxyhydroxysulfate mineral) through a biological method for the adsorption of arsenic and achieved 110 and 115 mg adsorptions of arsenic per gram of adsorbent for As (III) and As (V), respectively. To enhance the removal efficiency, some researchers added artificial ingredients to form synthetic materials as adsorbents and achieved excellent removal efficiencies [3,7,14,15]. Among these studies, Khan and Imteaz [14] used iron oxide-coated sand (IOCS) for the adsorption of arsenic and achieved up to 100% removal of arsenic with a higher dose of adsorbent.

Although many researchers proposed many different synthetic materials for effective arsenic removal, the preparation of most of those synthetic materials is costly exercise and, in many cases, not feasible for the distant poor communities who need the treatment for their daily potable water. It is highly recommended that for such communities, locally available natural materials be explored for such water treatments. As in the contemporary world, the focus on sustainability is gaining increasing momentum, recent studies focused on different types of natural sorbents, and even some by-products and/or waste materials from other processes. Villela-Martínez et al. [16] demonstrated that commercially produced bone char prepared from animal bones acts as an excellent adsorbent for removing arsenic from water. Byambaa et al. [17] used special adsorbent material (containing Fe and Al) commercially produced from acid mine drainage sludge for the removal of arsenic from water. Some other researchers also investigated the use of recycled material for arsenic adsorption [18–20]; however, they have used different synthetic chemicals for the transformation of the raw materials used, which is a cost burden for many communities and requires strict quality assurance. Moreover, using such recycled materials and/or industry by-products as filter materials for potable water requires thorough chemical investigations for any potential pollutants present in the recycled/waste material, which may leach from the used recycled/waste material and cause other health hazards for the consumers. Many countries implement stringent conditions on using such materials. As such, to avoid higher costs of treatment as well as strict regulations from relevant authorities, locally available filter media made from sand or ceramic are preferred and this concept resulted in several studies with locally available sand/ceramic filter media. However, the clear majority of the studies on arsenic removal with natural adsorbents were conducted through batch experiments [3,12–14,16,19–21]. Often the same adsorbents within a prototype-sized filter under a practical demand scenario exhibited lower removal efficiency compared to the efficiency obtained through the batch experiment.

A crucial issue of any such filter media is clogging; under continuous operation, the removal efficiency deteriorates due to clogging, which can be attributed to the iron present in the water, especially for groundwater. Usually, groundwater contains a considerable amount of iron, which is a major concern for the maintenance of adequate flow in any filter system for arsenic removal. Iron in groundwater is usually present as Fe (II) form and is soluble in this form [22]. However, when groundwater is withdrawn and comes into contact with oxygen, the Fe (II) is oxidised to Fe (III) depending on the availability of oxygen and the pH of the water [22]. Fe (III) oxide is insoluble and forms iron flocs that can block the filtration path in the filter column [23]. Consequently, filter systems for arsenic removal fail due to hydraulic incapacity rather than adsorption incapacity [24]. Hence, the success of any arsenic removal filter system is linked with the effective removal of iron

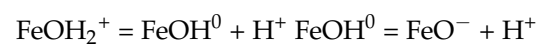
under real field conditions. Khan and Imteaz [12], after conducting detailed studies using batch experiments with six different types of natural adsorbents, concluded that locally (Australia) available Skye sand has the highest arsenic removal capacity. Although many such proposed filters were successful in removing arsenic to an excellent level through batch or column experiments, they were not suitable for a considerable period in a real-life scenario due to clogging and/or other side effects. Only testing with a prototype filter for a considerable period can ascertain the success of this type of filter. To investigate the arsenic and iron removal efficiencies of the mentioned Skye sand under practical conditions, this study describes detailed prototype experiments with the Skye sand.

2. Adsorption Chemistry

Adsorption is a mass transfer process, where a dissolved substance is transferred from the liquid phase to the surface of a solid material and becomes bound by chemical or physical forces. Once the adsorbate reaches the surface, another mechanism is required to promote attachment to the surface. The main mechanisms for the attachment of the adsorbate to the adsorbent surface are: (i) electrostatic attraction, through Coulombic forces; (ii) surface complexation reactions; and (iii) surface precipitation reactions.

2.1. Electrostatic Attraction

Electrostatic attraction is a physical process in which the ions are adsorbed to the oxide surface, which is oppositely charged. The surface charge of hydrous ferric oxide is the result of acid–base equilibria. It is a function of pH and of the ionic strength of the solution. The surface charge of hydrous ferric oxide may be positive (acidic), negative (basic) or zero (neutral) depending on gain or loss of proton. This can be expressed as:

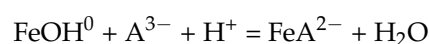
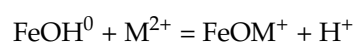
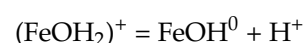


where $(\text{FeOH}_2)^+$, FeOH^0 and FeO^- represent hydrous ferric oxide surfaces, positively charged, neutral and negatively charged, respectively. If arsenic acid (H_3AsO_4) loses a proton (H^+), the remaining part of the molecule has a negative charge. At neutral pH, which is common for natural waters, arsenic acid loses one or two H^+ ions, giving the rest of the molecule a charge of -1 or -2 (H_2AsO_4^- or HAsO_4^{2-}).

Evidently, anions (negatively charged arsenic species) can be easily adsorbed with electrostatic forces to the hydrous iron oxide surface at a pH less than 8.0, and cations (positively charged arsenic species) at pH values greater than 8.0. This is the main reason for the high As (V) removal by iron-coated sand since the arsenic species related to As (V) exist as mono or divalent negatively charged ions at a pH less than 8 where the iron oxide surface is positively charged.

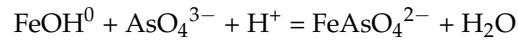
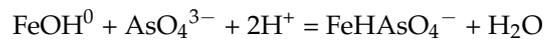
2.2. Surface Complexation

Hydrous ferric oxide ($\text{Fe}_2\text{O}_3 \cdot n\text{H}_2\text{O}$, n varying from 1 to 3) has reactive surface sites. Hydroxyl groups that coordinate and dissociate protons during adsorption process are replaced by adsorbed anions and cations. This was described by chemical equations for a divalent cation, M_2^+ , and a hypothetical trivalent anion, A_3^- , as follows:

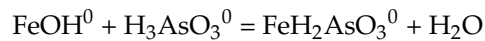


The adsorption of cations is favored at high pH values, while the adsorption of the anion is favored at low pH values, as can be observed from the above equations.

Pentavalent arsenate As (V) species are AsO_4^{3-} , HAsO_4^{2-} , $\text{H}_2\text{AsO}_4^{1-}$, and H_3AsO_4 . The surface complexation reaction for arsenate (AsO_4^{3-}) can be written as follows:

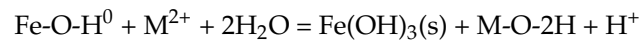


Since arsenite possesses neutral charge at pH values less than 9.2, it forms a neutral complex with hydrous ferric oxide as follows:

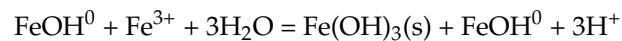


2.3. Surface Precipitation

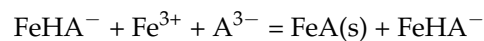
At higher concentrations, anions and cations can transfer from liquid to solid surfaces (iron oxide) by surface precipitation, which dominates over surface complexation. The governing chemical equations for cation surface precipitation are as follows:



and for anion surface precipitation are as follows:



Or,



Either in cation surface precipitation or in anion surface precipitation, a solid hydroxide species and a new surface phase (hydroxyl groups) species are formed. The hydroxyl groups allow a continuum between the adsorption and the precipitation of the adsorbing ions.

3. Methodology

A commercially available Skye sand sample was collected from a garden supplier located at Cranbourne, Victoria (Australia). Figure 1 shows the photo of the sample at the supplier's site. Prior to conducting arsenic adsorption experiments, several physical properties of the Skye sand samples was established through specific surface area (i.e., Brunauer–Emmett–Teller surface area), XRF, XRD, SEM and TEM analyses. It is to be noted that some of these tests with the same sample were mentioned in detailed in some earlier publications of the same authors [12,14].



Figure 1. Skye sand sample at the supplier's site.

Earlier, a prototype arsenic removal filter referred to as the 3rd Generation IHE Family Filter using iron oxide-coated sand (IOCS) as filter media was introduced by the UNESCO-IHE, Institute for Water Education, Delft, The Netherlands [23]. Laboratory experiments along with continuous field testing for four years revealed that this prototype filter could consistently produce iron- and arsenic-free water [25]. Additionally, it was found that regular draining in combination with occasional flushing of the filter was sufficient to maintain its hydraulic capacity [23,25].

However, in the earlier developed filter system with IOCS, the manganese concentration in the filtrate of 9 filters (out of 12) was much higher (1.5–12 times) than the manganese concentration of feed water. The increased concentration of manganese in the filtrate was likely due to release of manganese from IOCS itself [23]. It should be noted that IOCS contained 25 mg/g of manganese [23]. The current study adopted the same prototype configuration, except with the Skye sand as filter media, which is likely to overcome the issue of manganese contamination from the filter media. The IHE Family Filter runs in an up-flow mode, which facilitates less likelihood of air entrapment in the filter bed. Moreover, as the filter is flushed in a down-flow mode by opening the valve at the bottom of the filter column, the flushing of the filter bed in an opposite direction of filtration was convenient and there was less or no likelihood of the contamination of the filter media. By draining the filter bed, air will be introduced into the filter bed. However, by restoring the filtration process in an up-flow mode, all air will easily escape from the filter bed.

3.1. Filter System Configuration

The earlier developed prototype filter [23] was replicated at the School of Chemistry, Monash University, Melbourne. The design and operation of the prototype filter were similar to that of the IHE Family Filter [23]. The main design criteria of the prototype filter was:

- (a) Ability to run under gravity as many places in rural areas of developing countries (where their source of water is contaminated with arsenic) do not have dependable electricity supply for the use of pump;
- (b) Ability to control flow of water in the filter media so that arsenic and iron can be removed effectively;
- (c) Ability to avoid air-trapping in the filter bed to ensure consistent flow rate;
- (d) Ability to produce 100 L/day arsenic-free water with a factor of safety of “2”, where 50 L/day is sufficient for drinking and cooking purposes for a typical family in rural areas of developing countries [23]; and
- (e) Ability to flush iron flocs by a down-flow mode.

The following materials were used to construct the current filter system:

- (a) Water bucket for feed water and filtrate (food grade plastic; 50 L capacity each);
- (b) Adsorbent (Skye sand of 11 kg, 7 L);
- (c) Perforated mild steel disk as the support at the bottom of filter column;
- (d) Provision of dead volume at the bottom of filter column;
- (e) Scoria, a coarse-grained aggregate at the bottom of the filter bed as supporting material;
- (f) Food grade plastic filter column (15 cm in diameter);
- (g) Connecting rubber/plastic tubes, control valves, and tap;
- (h) Drain valve at the bottom of the filter for flushing/cleaning the filter bed; and
- (i) Mild steel frame for holding the water buckets.

The schematic diagram is shown in Figure 2 and the real prototype filter is illustrated in Figure 3. The feed water bucket was held on the top of filter column by the steel frame. It was connected by an inlet tube to the lower portion of the filter column. The flow is controlled by an orifice in the inlet tube.

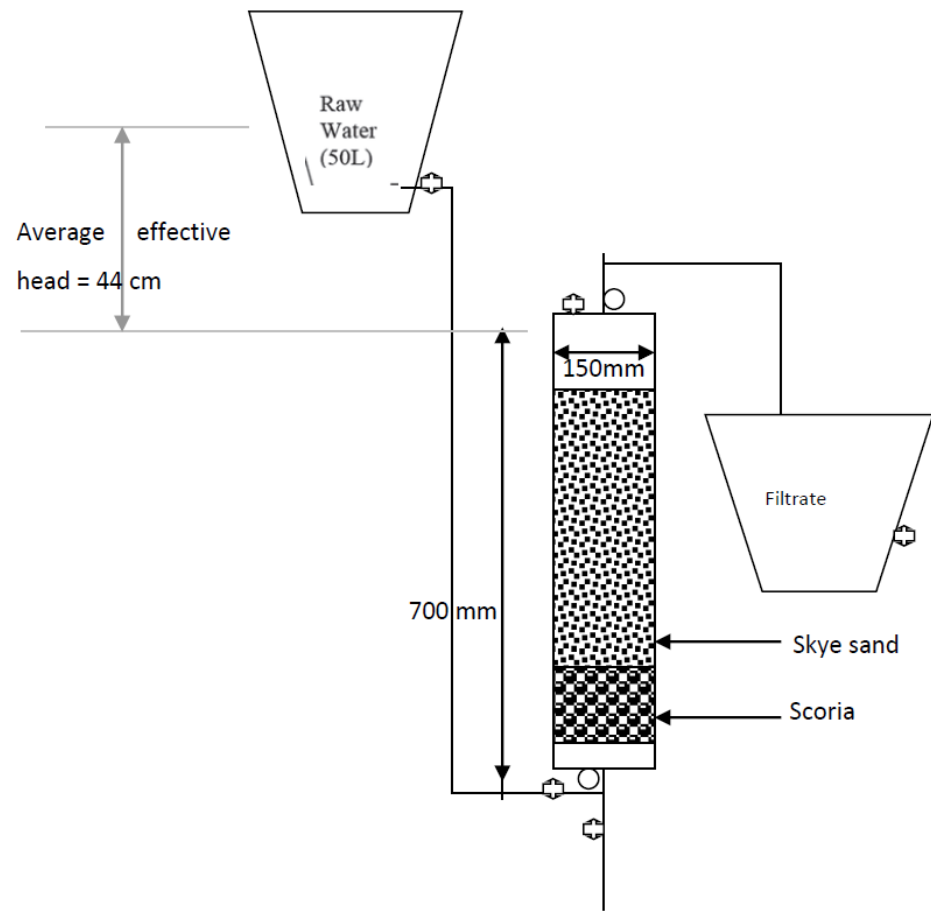


Figure 2. Schematic diagram of the prototype filter with Skye sand.

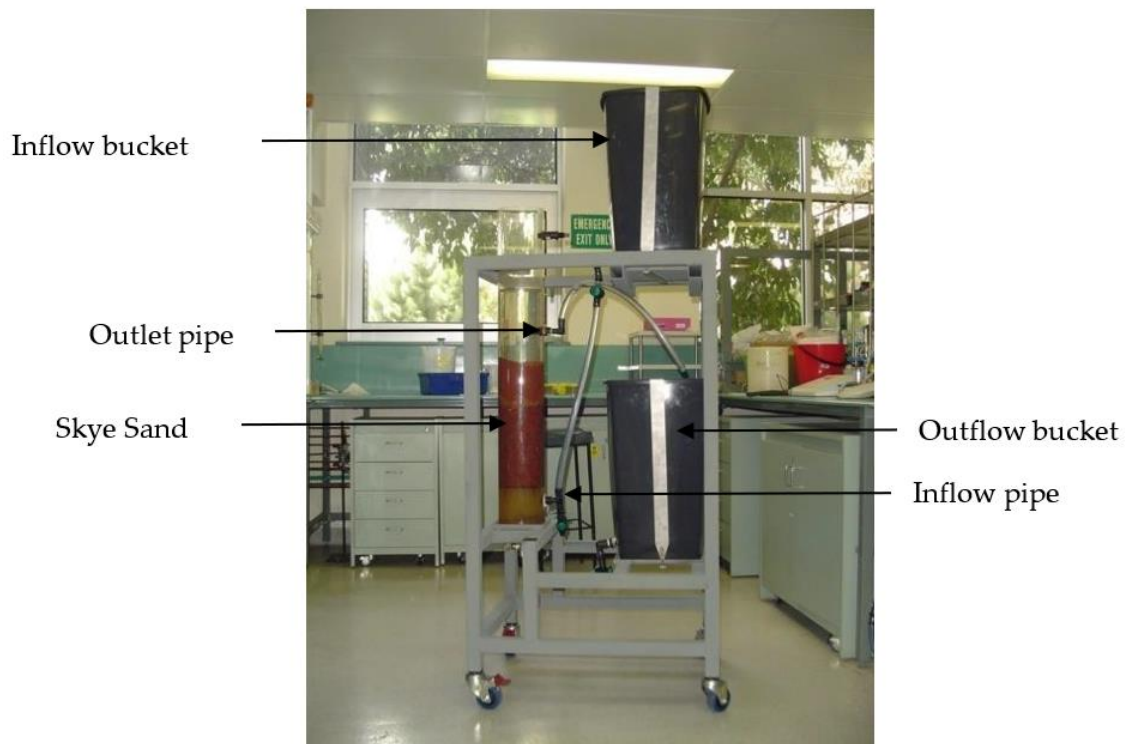


Figure 3. The prototype filter in the laboratory.

3.2. Filter Hydraulics

The established hydraulic parameters of the filter column are as follows:

- (a) Flow system: It is an up-flow system, i.e., feed water enters from the bottom of the filter bed and treated water comes out from the top of the filter bed. The feed water bucket, the filter bed and filtrate outlet are arranged in such a way that there is always at least 150 mm water column on the top of the filter bed. This prevents air entrapment in the filter bed. Both the feed-water bucket and the filter column are at atmospheric pressure.
- (b) Hydraulic head: The hydraulic head is the difference between the surface of water in the top bucket and the outlet for treated water in the filter column. During the filtration process, the level of the water surface of the top bucket decreases gradually. So, the hydraulic head is variable, typically from 36 to 52 cm.
- (c) Control of flow: Flow is controlled through the orifice in the inlet tube. Orifice sizes of 0.8 and 0.9 mm were tested at different hydraulic head. Finally, a 0.9 mm size was used in the prototype filter.
- (d) Cleaning of filter: A drainage valve was fitted at the bottom of the filter column for the cleaning/flushing of the filter bed in a down-flow mode. For operational convenience, the filter was cleaned once per week by opening the drain valve.

3.3. Scanning Electron Microscopy (SEM) and Transmission Electron Microscopy (TEM) Analyses

For SEM and TEM analyses, one sample from original Skye sand and one from arsenic-treated Skye sand in the filter prepared. These samples were mechanically crushed before sent to Monash Centre for Electronic Microscopy for SEM and TEM analysis. A JEOL JSM-7001F (Tokyo, Japan) in conjunction with a Bruker 10 mm² Si drift detector were used to investigate the microstructure and the elemental composition of Skye sand before and after being treated with As. The SEM was operated in an accelerating voltage of 15 kV, working distance of 10 mm and with an intermediate probe current to generate back scattered electron imaging (BSEI). BSEI was used to distinguish the variations in the composition of samples. Qualitative energy dispersive X-ray spectroscopy (EDS) was performed by using a large probe current, an accelerating voltage of 15 kV and analytical working distance of 10 mm. By collecting EDS spectra from a series of pixels across the sample surface 2D maps were constructed (TIF images). Spatial distributions of specific elements in the samples are shown in the TIF images.

3.4. Chemicals for Water Quality Testing

Arsenic standard solution (1000 mg/L As in nitric acid), sodium arsenite (NaAsO₂), iron standard solution (1000 mg/L Fe in nitric acid) and FeCl₃·6H₂O were purchased from Sigma Aldrich Pty Ltd., Australia. Arsenic was in the trivalent form both in the standard solution and NaAsO₂. Standard solutions were used as standards for the determination of arsenic and iron by EPA Method 1632 [26] using Hydride Generation-Atomic Absorption Spectroscopy (HG-AAS). Deionised water (DI) was used for the preparation of stock solutions and for dilution of both standard and stock solutions. Arsenic stock solutions (1000 mg/L) were prepared by dissolving 0.867 g of NaAsO₂ in 500 mL DI water. Iron stock solution (1000 mg/L) was prepared by dissolving 4.84 g of FeCl₃·6H₂O in 1000 mL DI water.

Melbourne tap water was characterised by Khan [27] as having the following properties: pH: 7.2–7.7; turbidity: 0.6–1.8 NTU; iron: 0.06 mg/L; manganese: 0.003 mg/L; arsenic: <5 µg/L; silica as SiO₂: 4.5 mg/L; total phosphorus: 7 µg/L; and total dissolved solids: 39 mg/L was used to prepare the feed water of the prototype filter column. Arsenic stock solution was added to the tap water to obtain 500 µg/L of arsenic in feed water. Moreover, iron stock solution was added to the water to obtain 3 mg/L of iron in feed water. The pH of feed water was adjusted to 6.9 and the temperature was 22 °C. At a pH > 3, the ferric form of iron is insoluble and presents as colloidal or suspended form. It was noted that a portion of the Fe(OH)₃ precipitated in the 50 L reservoir. However, as the oxidation rate

of iron only by dissolved oxygen in water is slow, a considerable portion of colloidal or suspended iron entered the filter column.

3.5. Flow Measuring Method

The flow from the system was measured using a 5 L measuring bucket after the water was collected at the outlet bucket. The hydraulic head is the difference between the surface of water in the top bucket and the outlet for treated water in the filter column. During the filtration process, the level of the water surface of the top bucket decreases gradually. So, the hydraulic head is variable, typically from 36 to 52 cm. The water flow was controlled by the hydraulic head and orifice in the inlet tube. With an orifice of 0.9 mm size, the flow rate varies from 3.83 to 4.67 L/h at different hydraulic heads.

3.6. Instruments and Methods for Chemical Analysis

For arsenic analysis, 50 mL of water samples were collected in a conical flask from an average volume of 50 L of filtrate from the prototype filter. Arsenic was analysed with an atomic absorption spectrometer (GBC, Model no. 906/AA) sourced from GBC (Melbourne, Australia) fitted with a hydride generation system (HG-AAS 3000). The parameters used for analysis of As by HG-AAS are: wavelength 193.7 nm, band pass 1.0 nm, lamp current 8.0 mA and fuel (acetylene) 1.3 L/min. The arsenic analysis method involves reacting the analyte in an acidified solution with sodium borohydride to form gaseous hydrides. 500 mL of sodium borohydride (NaBH_4) reagent solution was prepared. 3.0 g powdered NaBH_4 and 3.0 g NaOH (laboratory reagent grade) were added to deionised water and made up to 500 mL. The solution was filtered into the HG 3000 borohydride reagent bottle. The other bottle of the HG 3000 instrument was filled with 500 mL of hydrochloric acid (3.0 M) for analysis of arsenic samples. The efficiency of the arsenic hydride (AsH_3) generation process depends strongly on the valence state of the As ions present. As (III) shows approximately twice the sensitivity of As (V). Therefore, if As (V) is present or the arsenic valence state is unknown, it is advisable to reduce the sample prior to the analysis. For this purpose, the sample (usually 50–100 mL) was acidified with concentrated HCl (3 M) to give a 20% v/v solution. KI, AR grade, was added to give 200 mg/L of KI solution. The samples were allowed to rest for one hour for completion of the reaction. For each set of samples, a calibration curve was obtained by measuring the absorbance of arsenic standards 0, 5, 10, 15, 20 and 25 $\mu\text{g/L}$.

For iron analysis, 50 mL of water samples were collected in a conical flask from an average volume of 50 L of filtrate from the prototype filter. For iron analysis by AAS, standard samples were prepared by diluting the iron standard solution in deionised water. For each set of samples of filtrate, a calibration curve was obtained by measuring the absorbance of iron standards (0, 1, 2, 4, 6 and 8 mg/L).

4. Results

4.1. Physical Properties

Among fundamental physical properties, through grain size distribution of the sample, it was found that the Skye sand has an effective diameter (d_{10}), uniformity coefficient (Cu) and coefficient of curvature (Cz) of 0.08 mm, 4.25 and 1.19, respectively. By definition, the d_{10} of a sample of sand means the 10 percentile size; similarly, d_{30} and d_{60} are the 30 percentile and the 60 percentile, respectively. Cu is defined as the ratio of d_{60}/d_{10} and Cz is defined as $(d_{30})^2/((d_{10})(d_{60}))$. Additionally, the porosity (Po) and specific density (γ) of the Skye sand were found to be “0.39” and “2.58”, respectively.

The specific surface area, i.e., BET surface area, and average pore size of the Skye sand were measured by nitrogen adsorption and desorption. Both the specific surface area and pore size of the Skye sand were found to be significantly high (surface area: 5.77 m^2/g and pore size: 15 nm), rendering it as a suitable adsorbent [14].

XRF analysis reveals that the major components of Skye sand are: SiO_2 92.1%, Fe_2O_3 2.13%, Al_2O_3 2.04% and TiO_2 0.29%. It is evident that the presence of a significant portion of silica (SiO_2) with iron oxide (Fe_2O_3) in the Skye sand accelerates arsenic adsorption [14].

XRD analysis reveals that the major components of minerals present in the Skye sand are: quartz 28%, haematite 20%, goethite 18% and kaolinite-montmorillonite 14%. This proportion indicates that the surface of Skye sand contains goethite, haematite and different types of clay minerals. The presence of goethite and haematite is indicative of the presence of Fe, predominantly as oxides, which helps in removing arsenic [14].

The details of the results and measuring methods regarding physical properties, XRF and XRD are provided in Khan and Imteaz [12].

An optical microscopic view of the Skye sand is shown in Figure 4. From the microscopic analysis of the Skye sand, it is evident that the reddish sand particles had a sub-rounded shape and there was a thin film of iron on the silica.

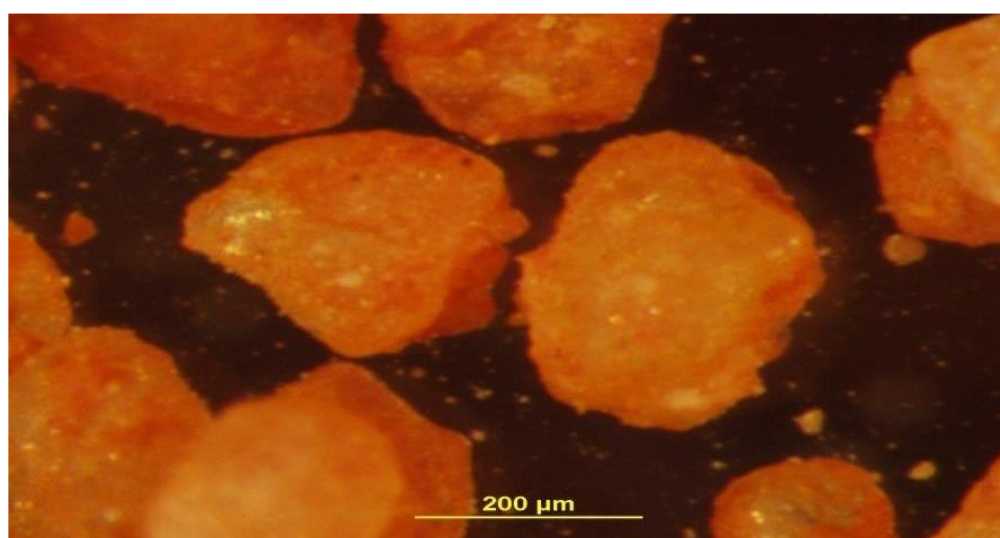


Figure 4. Optical microscopic view of the untreated Skye sand.

4.2. Flow of Water from the Filter

The prototype filter was operated in the laboratory with a capacity of approximately 52 L of filtrate per 12 h. The water flow was controlled by the hydraulic head and orifice in the inlet tube. With an orifice of 0.9 mm size, the flow rate varies from 3.83 to 4.67 L/h at different hydraulic head, while with an orifice of 0.8 mm size, the flow rate varies from 3.42 to 4.25 L/h. The hydraulic head varies from 36 to 52 cm in both cases and the average effective head was 44 cm. An orifice of 0.9 mm size was, therefore, used in the operation of the prototype filter. With this orifice, on average, 100 L of water was delivered in 24 h.

4.3. Filter Clogging and Recovery of Hydraulic Capacity

The filter was operated for 12 h per day for 21 days. The collected filtrate was 50 L on average. The mass of Skye sand in the filter column was 11 kg, with a volume of 7 L. Therefore, the prototype filter produced an approximately 7 bed volume (BV) of filtrate per 12 h. As iron and arsenic were present in the feed water, the deposition of iron flocs occurred at the bottom of the filter bed. Due to the deposition of iron flocs on the surface of Skye sand, the flow rate of the filter decreased over time. For operational convenience, the filter bed was flushed with water present in the filter column by opening the drain valve once per week. The flushing water coming down from the opposite direction through the filtration path removed most of the iron flocs which were attached to scoria and Skye sand. Consequently, the filter capacity was restored fully. The flow capacity of the filter was measured daily at a hydraulic head of 52 cm to study the variation of capacity over time. Moreover, the flow rate was measured before and after the flushing at a hydraulic

head of 52 cm. The flow rate reduction in the filters over one week of operation, as shown in Figure 5, was 14 to 16%. However, after flushing, the filter capacity returned to more than 99% of its original flow rate.

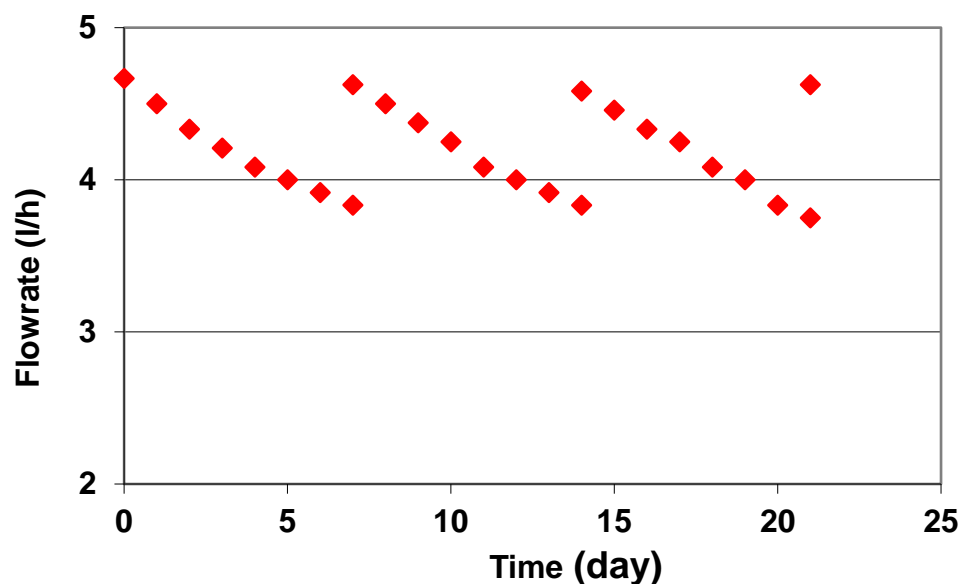


Figure 5. Flowrate reductions over time and subsequent recovery after flushing.

4.4. Arsenic and Iron Removal Performances

For the arsenic and iron removal experiments, the synthetic contaminated water was prepared with As = 500 $\mu\text{g/L}$ and Fe = 3.0 mg/L (resembling some highly contaminated water in south-east Asia). The contact time for filtration was 40 min and the filter was drained/flushed every 7 days as mentioned in the preceding section. The filter removed arsenic consistently to a level below the detection limit (0.05 $\mu\text{g/L}$). The same performance was achieved up to 150 bed volumes (1050 L) of filtrate. As such, it can be concluded that a complete removal of arsenic was achieved with the prototype filter for a considerable testing period. It was established through earlier batch experiments [12] that the arsenic adsorption capacity of the studied Skye sand is 2.73 mg/g. The current filter has a mass of 11 kg Skye sand, which is capable of adsorbing 30 g As. If the feed water arsenic concentration is 500 $\mu\text{g/L}$ and the filter is required to treat 100 L/day, arsenic adsorption per day would be 50 mg. As such, the current prototype filter with Skye sand can produce arsenic-free water continuously for 600 days (100 L per day) where the inflow arsenic concentration is 500 $\mu\text{g/L}$. Moreover, it is expected that the inflow water iron will add extra lifetime to the filter for arsenic removal due to added coating of iron oxide on the surface of Skye sand by the inflow water.

In regard to iron removal from the water, it was found that the filter removed iron consistently to a level below the WHO-acceptable limit of 0.3 mg/L. Additionally, the same filter performance was achieved up to a 150 bed volume (1050 L) of inflow water. As such, it can be concluded that complete iron removal was achieved with the prototype filter throughout the testing period.

4.5. Specific Surface Area and Pore Size Analysis

Figure 6 shows the relationship between pore volume and relative pressure for the Skye sand. The presence of a clear hysteresis loop indicates the existence of magnetic properties and mesoporosity (pores with diameters between 2 and 50 nm) on the surfaces of Skye sand. This attribute renders it to be a very good adsorbent.

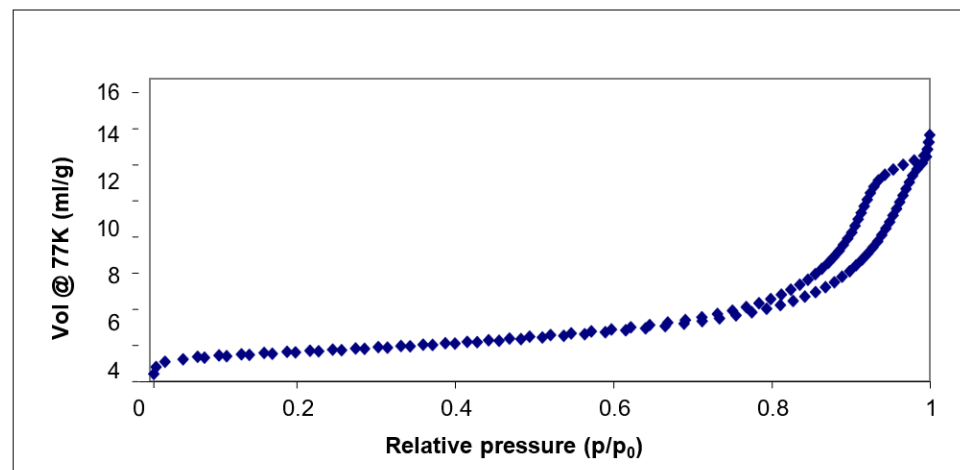


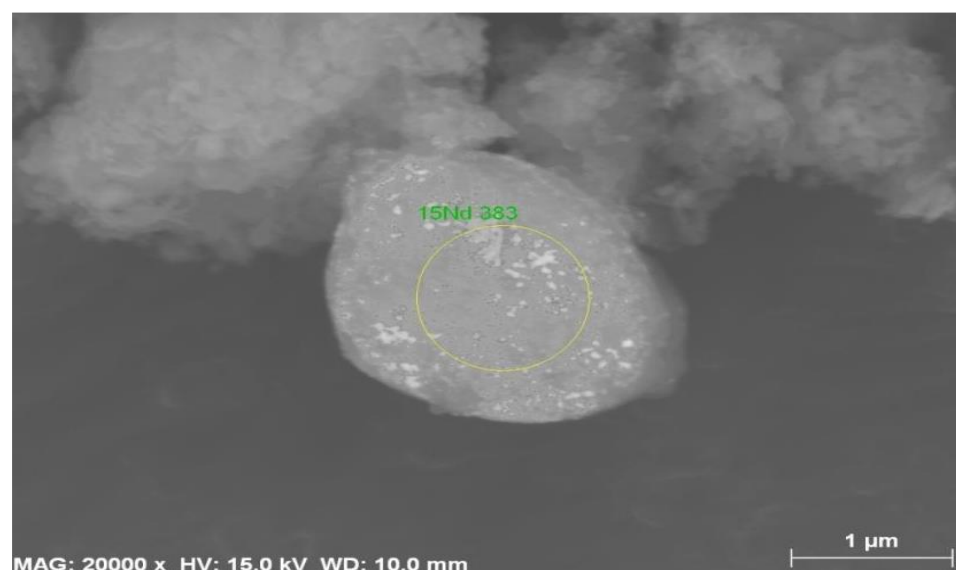
Figure 6. Analysis of the specific surface area of Skye sand.

4.6. SEM and EDX Analyses Results

Back-scattered electrons imaging (BSEI) processed from SEM analysis of Skye sand samples before and after arsenic adsorption are shown in Figure 7a,b, respectively. From the figures, a significant difference is observed in the arsenic-treated sample (Figure 7b).

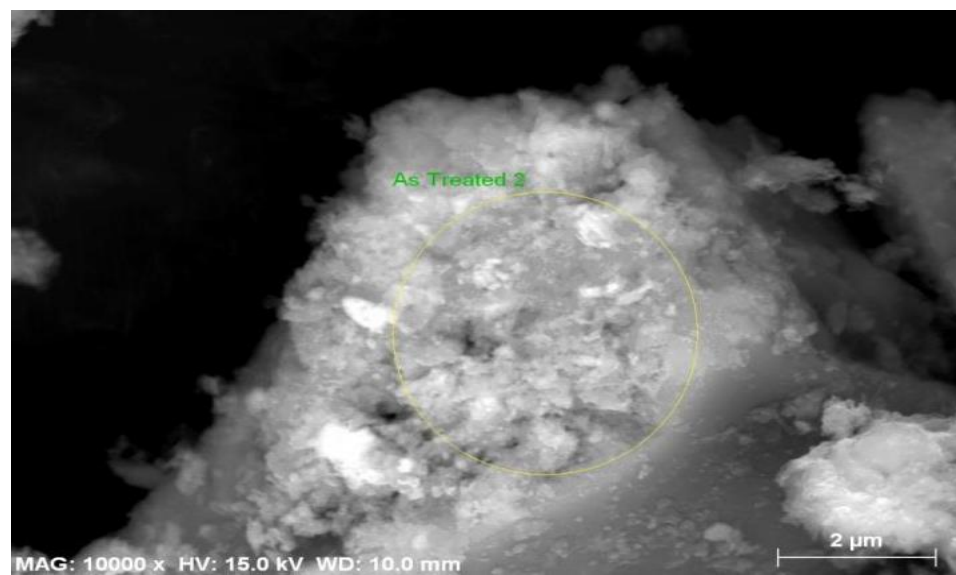
Energy dispersive x-ray spectra (EDXS) processed from TEM analysis of Skye sand samples before and after treatment are shown in Figure 8a,b, respectively. Different elements observed in Figure 8a are Al, Si, O, Fe, Mg, Ti and K, whereas different elements observed in Figure 8b are Al, Si, O, Fe, Mg, Ti, K and As. From the figures, it is evident that As has been adsorbed in the treated sample.

By collecting the EDXS spectra from a series of pixels across the sample surfaces of both original Skye sand and arsenic-treated Skye sand, 2D maps were reconstructed as TIF (Tagged Image Format) images. These reconstructed 2D maps (TIF images) show the spatial distribution of specific elements of the samples. The images are shown in Figure 9a (for original Skye sand) and Figure 9b (for treated Skye sand). The distribution of Si, Al and Fe is homogeneous in the TIF image of fines of original Skye sand (Figure 9a). The arsenic locations shown in Figure 9b are the places where Al and Fe are located in Figure 9a. The TIF images indicate that the regions containing Fe and the clay minerals containing Al are strongly associated with arsenic adsorption of Skye sand.



(a)

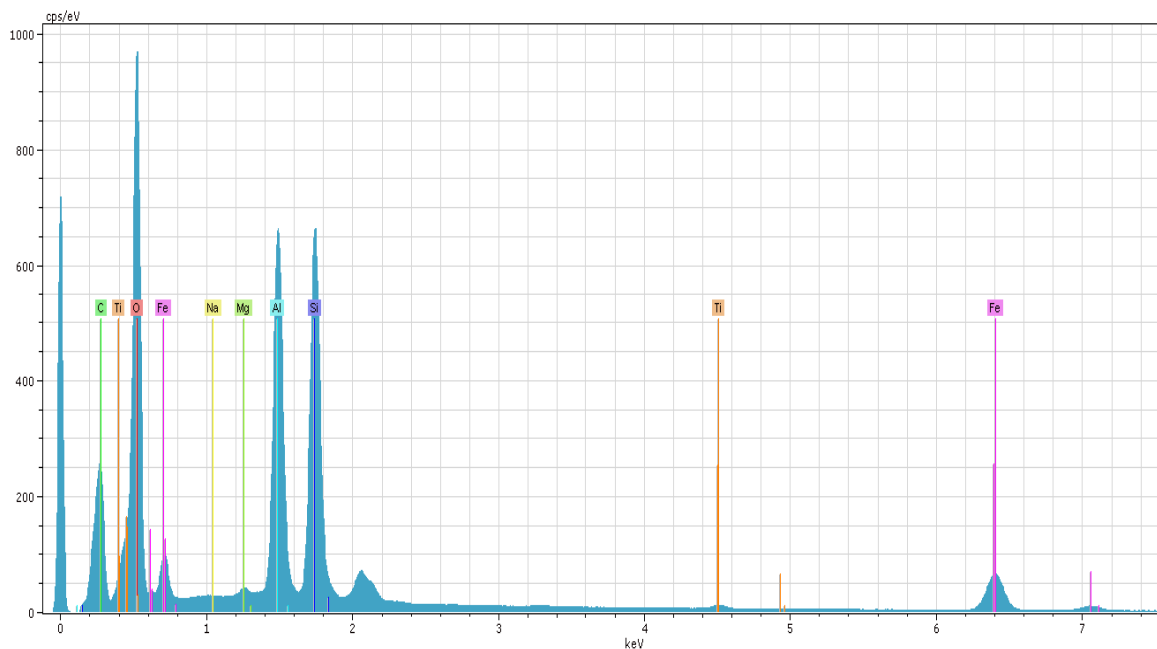
Figure 7. Cont.



(b)

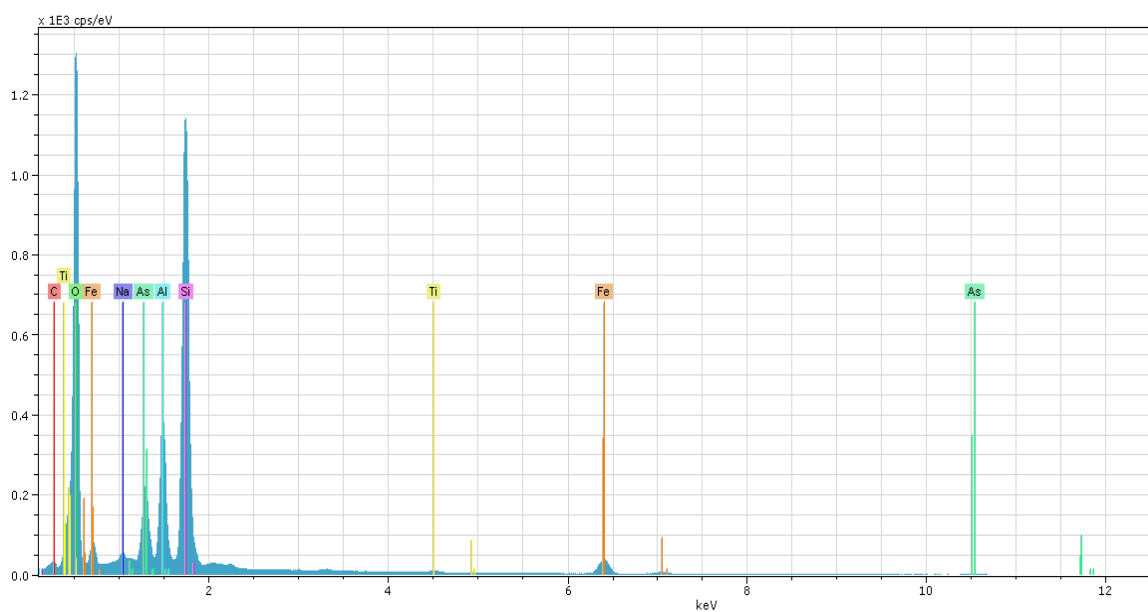
Figure 7. BSEI image of fines of (a) original Skye sand and (b) Skye sand after treatment.

It is to be noted that the source of the untreated Skye sand and arsenic-treated Skye sand is the same, the same bag of Skye sand. Therefore, their elemental distributions should be reasonably identical. However, the spatial distribution of the elements must be different in two different samples. The difference in the spatial distribution of the two different samples is made identical by TIF image processing, which renders the identical spatial distribution of elements facilitating signs of any treatment to the samples.



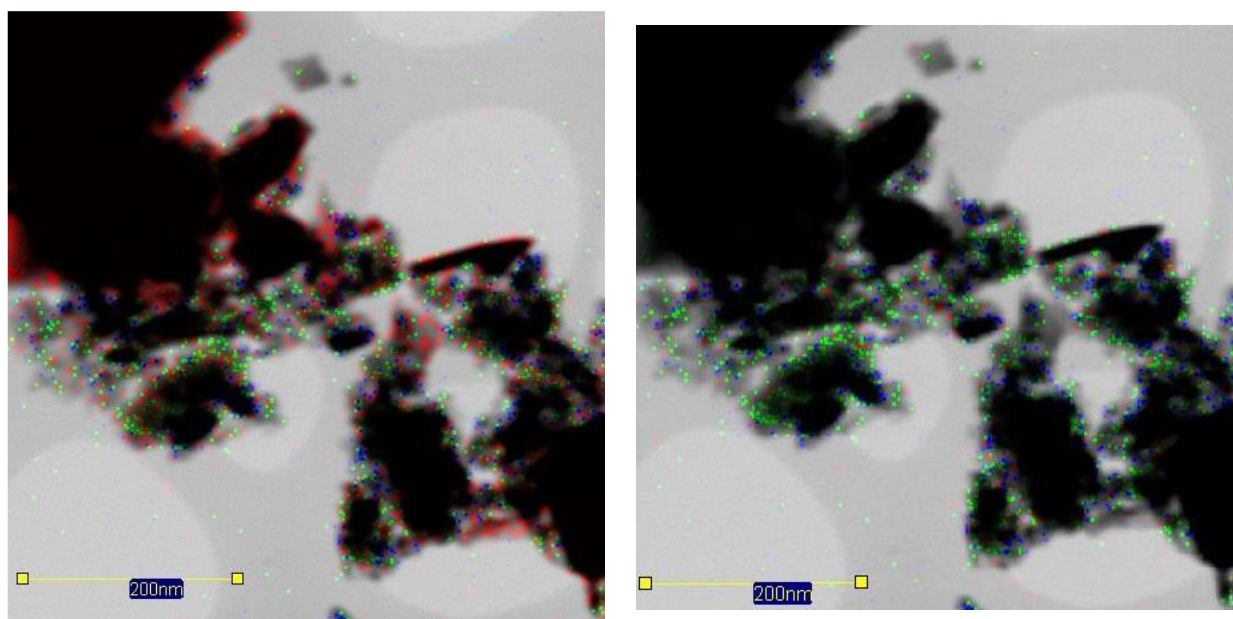
(a)

Figure 8. Cont.



(b)

Figure 8. EDXS spectra of fines of (a) original Skye sand and (b) Skye sand after treatment.



(a)

(b)

Figure 9. (a) Reconstructed 2D maps of EDXS of fines of original Skye sand (Si: red, Al: blue and Fe: green); (b) reconstructed 2D maps of EDXS fines of arsenic-treated Skye sand (As: red, Al: blue and Fe: green).

Mössbauer spectral analysis of the same samples [28] showed that among the iron oxides, only goethite contributed to the adsorption of arsenic. It should be noted that Mössbauer spectral analysis is limited to the determination of arsenic adsorption by iron oxides. For compatibility with the TEM elemental distribution (Figure 8b) and the TIF image of the arsenic-treated sample (Figure 9b), it can be interpreted that either goethite, or both the goethite and clay minerals, contributed to the deposition of arsenic on the surface of Skye sand.

5. Conclusions

Through batch and column experiments, Skye sand was found to be very effective in removing arsenic from water; however, this was never tested with a prototype system. The current prototype filter with the same Skye sand achieved very effective removal of arsenic up to a level below the arsenic detection limit ($0.05 \mu\text{g/L}$) and this performance was maintained for a considerable period of up to 150 bed volumes, i.e., 1050 L. As arsenic-contaminated water is often associated with iron, which causes early clogging of the filter system, the current filter system had a secondary objective of removing iron from the water. It was found that the current prototype is also capable of removing iron to the WHO-acceptable limit (0.3 mg/L). Achieving this secondary objective ascertains that the filter system is capable of maintaining its efficiency for a longer period compared to an earlier proposed filter system using IOCS developed at the UNESCO-IHE Institute for Water Education, The Netherlands. Analytical calculation suggests that the current filter is capable of treating arsenic-contaminated water, achieving arsenic-free water, continuously for 600 days at a rate of 100 L/day, where the feed arsenic concentration is $500 \mu\text{g/L}$. Additionally, it satisfies the hydraulic requirements; the contact time of the filtrate in the filter bed was 40 min, which indicates that Skye sand is a more efficient adsorbent than IOCS used in the IHE Family Filter. The flow rate reductions in the current filter over one week of operation were found to vary from 14 to 16%. However, after backwashing, the filter capacity returned to more than 99% of its original flow rate, which was not the case for the IHE filter using IOCS. Additionally, the current filter overcomes the drawback of the IHE Family Filter, which releases manganese (Mn) in the filtrate due to a high Mn content (25 mg/g) in the IOCS. As Skye sand has a very low manganese content (0.8 mg/g), the current filter does not release Mn in the filtrate. SEM and TEM analyses of the Skye sand samples after and before treatment confirm the trapping of As and Fe on the sand surface.

The same filter has the potential of removing other harmful heavy metals, which is a concern for potable water sources in many regions. However, this needs to be ascertained by further experiments targeting some of those harmful heavy metals. For the current study, this was out of the scope. After operations of longer periods, the sand in the filter will require replacement, which is likely to generate sludge. With the aim of recycling, such sludge (i.e., contaminated sand) can be used in concrete for building construction.

Author Contributions: Project administration, supervision, and writing this paper, M.A.I.; experimental data collection and analysis, S.A.K. All authors have read and agreed to the published version of the manuscript.

Funding: This research received no external funding.

Data Availability Statement: Data are available from the first author upon request.

Conflicts of Interest: The authors declare no conflict of interest.

References

1. Ahmad, A.; van der Wens, P.; Baken, K.; de Waal, L.; Bhattacharya, P.; Stuyfzand, P. Arsenic reduction to $<1 \mu\text{g/L}$ in Dutch drinking water. *Environ. Int.* **2020**, *134*, 105253. [[CrossRef](#)] [[PubMed](#)]
2. Maity, J.P.; Nath, B.; Kar, S.; Chen, C.Y.; Banerjee, S.; Jean, J.-S.; Liu, M.-Y.; Centeno, J.A.; Bhattacharya, P.; Chang, C.L.; et al. Arsenic-induced health crisis in peri-urban Moyna and Ardebok villages, West Bengal, India: An exposure assessment study. *Environ. Geochem. Health* **2012**, *34*, 563–574. [[CrossRef](#)] [[PubMed](#)]
3. Pizarro, C.; Escudey, M.; Caroca, E.; Pavez, C.; Zúñiga, G.E. Evaluation of zeolite, nanomagnetite, and nanomagnetite-zeolite composite materials as arsenic (V) adsorbents in hydroponic tomato cultures. *Sci. Total Environ.* **2021**, *751*, 141623. [[CrossRef](#)] [[PubMed](#)]
4. Mohan, D.; Pittman, C.U. Arsenic removal from water/wastewater using adsorbents—A critical review. *J. Hazard. Mater.* **2007**, *142*, 1–53. [[CrossRef](#)]
5. Sakr, A.K.; Abdel Aal, M.M.; Abd El-Rahem, K.A.; Allam, E.M.; Abdel Dayem, S.M.; Elshehy, E.A.; Hanfi, M.Y.; Alqahtani, M.S.; Cheira, M.F. Characteristic Aspects of Uranium(VI) Adsorption Utilizing Nano-Silica/Chitosan from Wastewater Solution. *Nanomaterials* **2022**, *12*, 3866. [[CrossRef](#)]

6. Boussouga, Y.A.; Frey, H.; Schäfer, A.I. Removal of arsenic(V) by nanofiltration: Impact of water salinity, pH and organic matter. *J. Memb. Sci.* **2021**, *618*, 118631. [[CrossRef](#)]
7. Goren, A.Y.; Kobya, M. Arsenic removal from groundwater using an aerated electrocoagulation reactor with 3D Al electrodes in the presence of anions. *Chemosphere* **2021**, *263*, 128253. [[CrossRef](#)]
8. Callegari, A.; Ferronato, N.; Rada, E.C.; Capodaglio, A.G.; Torretta, V. Assessment of arsenic removal efficiency by an iron oxide-coated sand filter process. *Environ. Sci. Pollut. Res.* **2018**, *25*, 26135–26143. [[CrossRef](#)]
9. Bora, A.J.; Gogoi, S.; Baruah, G.; Dutta, R.K. Utilization of co-existing iron in arsenic removal from groundwater by oxidation-coagulation at optimized pH. *J. Environ. Chem. Eng.* **2016**, *4*, 2683–2691. [[CrossRef](#)]
10. Choong, T.S.Y.; Chuah, T.G.; Robiah, Y.; Koay, F.L.G.; Azni, I. Arsenic toxicity, health hazards and removal techniques from water: An overview. *Desalination* **2007**, *217*, 139–166. [[CrossRef](#)]
11. Murugesan, G.S.; Sathishkumar, M.; Swaminathan, K. Arsenic removal from groundwater by pretreated waste tea fungal biomass. *Bioresour. Technol.* **2006**, *97*, 483–487. [[CrossRef](#)] [[PubMed](#)]
12. Khan, S.A.; Imteaz, M.A. Experimental studies on arsenic removal efficiencies through adsorption using different natural adsorbents. *Water Air Soil Pollut.* **2021**, *232*, 16. [[CrossRef](#)]
13. Xiong, H.; Hu, D.; Shi, K.; Zhu, S.; Xu, Y. Adsorptive removal of arsenic ions from contaminated water using low-cost schwertmannites and akaganéites. *Mater. Chem. Phys.* **2023**, *297*, 127411. [[CrossRef](#)]
14. Khan, S.A.; Imteaz, M.A. Batch experiments on arsenic removal efficiencies through adsorption using synthetic and natural sand samples. *Int. J. Environ. Sci. Technol.* **2021**, *18*, 2357–2364. [[CrossRef](#)]
15. Yao, S.; Liu, Z.; Shi, Z. Arsenic removal from aqueous solutions by adsorption onto iron oxide/activated carbon magnetic composite. *J. Environ. Health Sci. Eng.* **2014**, *12*, 58. [[CrossRef](#)]
16. Villela-Martínez, D.E.; Leyva-Ramos, R.; Aragón-Piña, A.; Navarro-Tovar, R. Arsenic elimination from water solutions by adsorption on bone char. Effect of operating conditions and removal from actual drinking water. *Water Air Soil Pollut.* **2020**, *231*, 201. [[CrossRef](#)]
17. Byambaa, E.; Seon, J.; Kim, T.H.; Kim, S.D.; Ji, W.H.; Hwang, Y. Arsenic (V) Removal by an Adsorbent Material Derived from Acid Mine Drainage Sludge. *Appl. Sci.* **2021**, *11*, 47. [[CrossRef](#)]
18. Zhang, W.; Singh, P.; Paling, E.; Delides, S. Arsenic removal from contaminated water by natural iron ores. *Miner. Eng.* **2004**, *17*, 517–524. [[CrossRef](#)]
19. Shaikh, W.A.; Alam, M.A.; Alam, M.O.; Chakraborty, S.; Owens, G.; Bhattacharya, T.; Mondal, N.K. Enhanced aqueous phase arsenic removal by a biochar based iron nanocomposite. *Environ. Technol. Innov.* **2020**, *19*, 100936. [[CrossRef](#)]
20. Zeng, H.; Zhai, L.; Zhang, J.; Li, D. As(V) adsorption by a novel core-shell magnetic nanoparticles prepared with Iron-containing water treatment residuals. *Sci. Total Environ.* **2021**, *753*, 142002. [[CrossRef](#)]
21. Saldaña-Robles, A.; Saldaña-Robles, A.; Márquez-Herrera, A.; Ruiz-Aguilar, G.M.D.L.; Saldaña-Robles, N. Adsorption of arsenic on granular ferric hydroxide (GEH[®]). Impact of initial concentration of arsenic(V) on kinetics and equilibrium state. *Environ. Prot. Eng.* **2018**, *44*, 51. [[CrossRef](#)]
22. Buamah, R.; Petrusevski, B.; Schippers, J.C. Oxidation of adsorbed ferrous iron: Kinetics and influence of process conditions. *Water Sci. Technol.* **2009**, *60*, 2353–2363. [[CrossRef](#)] [[PubMed](#)]
23. Khan, S. Field-Testing of Improved IHE Family Filter in Bangladesh. Master's Thesis, UNESCO-IHE Institute for Water Education, Delft, The Netherlands, 2004.
24. Deliyanni, E.; Bakoyannakis, D.; Zouboulis, A.; Matis, K. Sorption of As(V) ions by akaganéite-type nanocrystals. *Chemosphere* **2003**, *50*, 155–163. [[CrossRef](#)] [[PubMed](#)]
25. Petrusevski, B.; Sharma, S.; van der Meer, W.G.; Kruis, F.; Khan, M.; Barua, M.; Schippers, J.C. Four years of development and field-testing of IHE arsenic removal family filter in rural Bangladesh. *Water Sci. Technol.* **2008**, *58*, 53–58. [[CrossRef](#)]
26. EPA. *Method 1632: Chemical Speciation of Arsenic in Water and Tissue by Hydride Generation Quartz Furnace Atomic Absorption Spectrometry*; Engineering and Analysis Division, U.S. Environmental Protection Agency: Washington, DC, USA, 1998.
27. Khan, S.A. Removal of Arsenic from Drinking Water by Natural Adsorbents. Ph.D. Thesis, Monash University, Melbourne, Australia, 2017.
28. Cashion, J.D.; Khan, S.A.; Patti, A.F.; Adeloju, S.; Gates, W.P. Mechanism of groundwater arsenic removal by goethite-coated mineral sand. *Hyperfine Interact.* **2017**, *238*, 101. [[CrossRef](#)]

Disclaimer/Publisher's Note: The statements, opinions and data contained in all publications are solely those of the individual author(s) and contributor(s) and not of MDPI and/or the editor(s). MDPI and/or the editor(s) disclaim responsibility for any injury to people or property resulting from any ideas, methods, instructions or products referred to in the content.